

# Comprehensive Report

---

## Laboratory evaluation of saw blades for cutting fiber-cement siding

Chaolong Qi, PhD, PE

Lieutenant, U.S. PUBLIC HEALTH SERVICE

Seungkoo Kang, PhD

---

Division of Applied Research and Technology  
Engineering and Physical Hazards Branch  
DART No. 19-114

May 2019



## **Disclaimer**

Mention of any company or product does not constitute endorsement by the National Institute for Occupational Safety and Health (NIOSH), Centers for Disease Control and Prevention (CDC).

In addition, citations to websites external to NIOSH do not constitute NIOSH endorsement of the sponsoring organizations or their programs or products. Furthermore, NIOSH is not responsible for the content of these websites. All Web addresses referenced in this document were accessible as of the publication date.

## Table of Contents

Disclaimer .....	2
Abstract .....	4
Introduction .....	6
Background for Control Technology Studies .....	6
Background for this Study .....	6
Materials and Methods in the Laboratory Evaluation .....	9
Laboratory Testing System .....	9
Saw blades for cutting fiber-cement.....	11
Test Conditions .....	14
Sampling Methods .....	16
Operating procedure for a cutting test.....	19
Results and Data Analysis for the Laboratory Evaluation .....	19
Discussion.....	24
Conclusions/Recommendations .....	25
References .....	26

## Abstract

Workplace exposure to respirable crystalline silica (RCS) can cause silicosis, a progressive lung disease marked by scarring and thickening of the lung tissue. Quartz is the most common form of crystalline silica. Crystalline silica is found in several construction materials, such as brick, block, mortar, and concrete. Construction tasks that cut, break, grind, abrade, or drill those materials have been associated with overexposure to dust containing RCS. Fiber-cement products can contain as much as 50% crystalline silica and cutting this material has been shown to cause excessive exposures to RCS. NIOSH scientists conducted this study to evaluate different saw blades for cutting fiber-cement siding, aiming at identifying blade design features that lead to lower dust generation and releasing.

Detailed characterizations of the dust generated from cutting fiber-cement siding using a circular saw with 22 different saw blades were conducted in a laboratory setting. The releasing rate of respirable dust, i.e.,  $G_{APS}$ , was analyzed and compared with and without engineering control measures for each blade. Two passive control measures were specifically evaluated. First, a dust-collecting box with a capped exhaust port was attached to the circular saw. Second, the dust-collecting box was connected to a passive dust collector, which includes a cyclone and a filter cartridge. Both control measures help collect a portion of the dust by the induced airflow from the spinning blade.

The  $G_{APS}$  generally increases with the number of teeth and the kerf width of the blades. The Plank Cutter<sup>®</sup> blade, which has a continuous rim of blade tips, generated the highest amount of dust in all three test conditions. The effect of the number of blade teeth was reduced when the passive dust control measures were used, possibly because more teeth may induce a higher airflow rate and generate more dust. Excluding the Plank Cutter<sup>®</sup> blade, the  $G_{APS}$  for the uncontrolled test condition ranges from 0.25 to 0.50 g/m, and reduces to 0.22-0.40 g/m with the capped dust-collecting box, and to 0.12-0.29 g/m when the passive dust collector was connected to the dust-collecting box. The 4-tooth Hitachi blade results in the lowest dust releasing rate under the testing conditions with both passive dust control measures, possibly due to fewer teeth, thinner kerf, and its specific design characteristics of a "smooth" gullet design for an optimized balance between inducing airflow and transporting the dust into the dust collectors.

Both passive dust control measures led to certain amounts of dust collection for most of the tested blades. The control measure with the passive dust collector provided a dust collection efficiency as high as 66% depending on the blade design. The gullet design of the blade seems to play an important role affecting the amount of dust releasing as well as the collection efficiency of the passive dust controls. Based on the exposure data from previous field surveys, additional improvement in blade designs might reduce the 8-hour time weighted average exposure to RCS below the NIOSH REL and OSHA PEL while cutting fiber-cement siding using a circular saw with passive on-tool dust collectors. Further investigation will be

needed to improve the blade design with the passive dust control measure, and to validate its performance through field studies.

## Introduction

### Background for Control Technology Studies

The National Institute for Occupational Safety and Health (NIOSH) is the primary Federal agency engaged in occupational safety and health research. Located in the Department of Health and Human Services, it was established by the Occupational Safety and Health Act of 1970. This legislation mandated NIOSH to conduct a number of research and education programs separate from the standard setting and enforcement functions carried out by the Occupational Safety and Health Administration (OSHA) in the Department of Labor. An important area of NIOSH research deals with methods for the identification, characterization and control of occupational exposures to potential chemical and physical hazards. The Engineering and Physical Hazards Branch (EPHB) of the Division of Applied Research and Technology has been given the lead within NIOSH to study the engineering aspects of health hazard prevention and control.

### Background for this Study

Crystalline silica refers to a group of minerals composed of silicon and oxygen; a crystalline structure is one in which the atoms are arranged in a repeating three-dimensional pattern [Bureau of Mines 1992]. The three major forms of crystalline silica are quartz, cristobalite, and tridymite; quartz is the most common form [Bureau of Mines 1992]. Respirable crystalline silica (RCS) refers to that portion of airborne crystalline silica dust that is capable of entering the gas-exchange regions of the lungs if inhaled; this includes particles with aerodynamic diameters less than approximately 10 micrometers ( $\mu\text{m}$ ) [NIOSH 2002]. Silicosis, a fibrotic disease of the lungs, is an occupational respiratory disease caused by the inhalation and deposition of RCS dust [NIOSH 1986]. Silicosis is irreversible, often progressive (even after exposure has ceased), and potentially fatal. Because no effective treatment exists for silicosis, prevention through exposure control is essential.

The NIOSH Recommended Exposure Limit (REL) sets an exposure limit for RCS of 0.05 milligrams per cubic meter ( $\text{mg}/\text{m}^3$ ) as a time-weighted average (TWA) determined during a full-shift sample for up to a 10-hour (hr) workday during a 40-hr workweek to reduce the risk of developing silicosis, lung cancer, and other adverse health effects [NIOSH 2002]. When source controls cannot keep exposures below the NIOSH REL, NIOSH also recommends minimizing the risk of illness that remains for workers exposed at the REL by substituting less hazardous materials for crystalline silica when feasible, by using appropriate respiratory protection, and by making medical examinations available to exposed workers [NIOSH 2002]. In March 2016, OSHA issued a new Permissible exposure limit (PEL) of 0.05  $\text{mg}/\text{m}^3$  for 8-hr TWA exposures [81 Fed. Reg.<sup>1</sup> 16285 (2016)]. The Threshold Limit Values<sup>®</sup> (TLVs<sup>®</sup>) recommended by the American Conference of Governmental Industrial Hygienists (ACGIH<sup>®</sup>) for  $\alpha$ -quartz and cristobalite (respirable fraction) is 0.025

---

<sup>1</sup> *Federal Register*. See Fed. Reg. in references.

mg/m<sup>3</sup> [ACGIH 2016]. The TLV is intended to mitigate the risk of pulmonary fibrosis and lung cancer. When dust controls are not used or maintained or proper practices are not followed, RCS exposures can exceed the NIOSH REL, the OSHA PEL, or the ACGIH TLV.

Crystalline silica is a constituent of several materials commonly used in construction, including brick, block, and concrete. Many construction tasks have been associated with overexposure to dust containing crystalline silica [Chisholm 1999; Flanagan et al. 2003; Rappaport et al. 2003; Woskie et al. 2002]. Among these tasks are tuckpointing, concrete cutting, concrete grinding, abrasive blasting, and road milling [Nash and Williams 2000; Thorpe et al. 1999; Akbar-Khanzadeh and Brillhart 2002; Glindmeyer and Hammad 1988; Linch 2002; Rappaport et al. 2003]. Fiber-cement products can contain as much as 50% crystalline silica. Cutting this material with power saws has been shown to cause excessive exposures to RCS [Lofgren et al. 2004; Qi et al. 2013].

The use of fiber-cement siding in construction and renovation is undergoing rapid growth. From 1991 to 2010, the market share of fiber-cement siding has climbed from 1% to 13% [US Census Bureau 2013]. In contrast, the market share of wood siding in residential construction has decreased from 38% to 8% [US Census Bureau 2013]. The durability and appearance of fiber-cement siding, which simulates wood without the maintenance issues associated with wood siding, is appealing and reportedly provides a competitive advantage over other building materials [Bousquin 2009]. The use of fiber-cement siding is expected to continue to increase. The number of workers exposed to dust containing crystalline silica as a result can also be expected to increase as the use of fiber-cement siding displaces other siding products. Cellulose fiber, sand or fly ash, cement, and water are the principal ingredients used in the manufacture of fiber-cement products.

Fiber-cement board is cut using three methods: scoring and snapping the board, cutting the board using shears, and cutting the board using power saws. When scoring and snapping the board, a knife is used to score the board by scribing a deep line into the board. The board is bent, and it breaks along the scored line. This method should be relatively dust-free. The score and snap method can be used when installing fiber-cement board used for tile underlayment, but is not applicable to siding. Commercially available tools used to shear fiber-cement siding include foot-powered shears and hand-held shears that may be manual or use a power source. Power saws, such as circular saws and compound miter saws, are used to cut fiber-cement siding. These saws are normally used with 4-8 tooth polycrystalline diamond-tipped (PCD) blades specifically designed to cut fiber-cement siding and minimize dust generation. Several commercially available saws are manufactured with hoods and exhaust take-offs that can be connected to vacuum cleaners or to dust-collection bags. These hoods partially enclose the saw blade. Available blade diameters are 5, 7.25, 10, and 12 inches (12.7, 18.4, 25.4, and 30.5 centimeter (cm), respectively).

For workers using power saws, the study by Lofgren et al. [2004] reported that their uncontrolled exposures to RCS ranged from 0.02 to 0.27 mg/m<sup>3</sup> during sampling, and their 8-hr TWA exposure ranged from 0.01 to 0.17 mg/m<sup>3</sup> depending on the length of exposure on the day sampled. The highest result was 3.4 times the NIOSH REL for RCS of 0.05 mg/m<sup>3</sup>. In an in-depth field survey, Qi et al. [2013] reported that a cutter's uncontrolled exposures to RCS ranged from 0.06 to 0.13 mg/m<sup>3</sup> when using power saws, and the 8-hr TWA exposure ranged from 0.02 mg/m<sup>3</sup> to 0.13 mg/m<sup>3</sup> depending on the length of exposure on the day sampled. The highest result was 2.6 times the NIOSH REL for RCS of 0.05 mg/m<sup>3</sup>.

The data from both field surveys suggested excessive exposures to RCS occurred when power saws without an engineering control were used for cutting fiber-cement siding. Qi et al. [2014] reported a simple and low cost engineering control achieved by attaching a regular shop vacuum to a dust-collecting circular saw for cutting fiber-cement siding. Three circular saws were evaluated in a laboratory study. All of them featured a built-in dust collection container or shroud, which served as a hood and partially enclosed the saw blade for collecting dust while cutting. The dust removal efficiency for the circular saws was greater than 78% even at a low flow rate of 0.83 m<sup>3</sup>/min [29 cubic feet per minute (CFM)] for the local exhaust ventilation (LEV) system used. The results from the laboratory evaluation suggested that connecting a dust-collecting circular saw to a basic shop vacuum with built-in air filters had the potential to provide a simple and low-cost engineering control measure for the dust generated from cutting fiber-cement siding. Four field surveys were conducted to validate the effectiveness of the engineering control measure suggested from the laboratory evaluation. The survey results from 21 full-shift samples showed that the 8-hr TWA exposure to RCS for the workers who mainly cut fiber-cement siding on the job sites was well under control, with a geometric mean of 0.011 mg/m<sup>3</sup> and the 95% upper confidence limit being only 30% of the NIOSH REL. This engineering control measure effectively reduced occupational silica exposures and provided an effective, simple and low cost solution for workers cutting fiber-cement siding.

In two of the four field surveys [Qi and Echt, 2014; Qi and Garcia, 2014], a prototype circular saw with an on-tool cyclone dust collector and an air filter was also evaluated. This prototype circular saw was developed by James Hardie Industries (Mission Viejo, CA) and referred to as the "red-spur saw" in the report by Qi et al. [2014]. The red-spur saw had a dust-collecting feature with a built-in shroud covering the saw blade. The shroud was connected to a cyclonic dust collector and a subsequent chamber which housed an air filter. When cutting fiber-cement siding, the flow induced by the spinning blade caused the shroud to collect a large portion of the dust generated when the fiber-cement was cut. The induced airflow also directed the dust through the cyclone and air filter, eliminating the need for an external dust collector or shop vacuum. The geometric mean and the 95% upper confidence limit of the RCS exposure from six full-shift (8-hr TWA) samples were 0.049 mg/m<sup>3</sup> and 0.105 mg/m<sup>3</sup>, respectively. During the surveys, PCD blades (Model D0704DH, Freud America, Inc., High Point, NC) with four teeth,



a diameter of 7.25 in (18.2 cm), and a kerf width of 0.071 in (1.8 millimeters (mm)) were used. The prototype was later commercialized by Roan Tools (MSEJH LLC, Bolingbrook, IL). It is likely that further improvements in saw blade designs may lead to lower exposures when using such dust-collecting saws by both reducing the dust generation and increasing induced flow and dust transportation into the on-tool dust collectors.

In this study, the dust generated from cutting fiber-cement siding using 22 different saw blades was evaluated and compared in a laboratory setting with and without dust control measures. The results can be used to identify saw blade designs with lower dust releasing rates and higher on-tool dust collection efficiencies, thus leading to lower exposure levels for workers cutting fiber-cement siding.

## Materials and Methods in the Laboratory Evaluation

### Laboratory Testing System

A worker's exposure to RCS during construction work can vary due to weather conditions, construction materials involved, work location, type of work performed, task duration and frequency, work practices, personal protective equipment (PPE), and whether or not dust control measures were used. Laboratory evaluation of dust generation and dust controls is an approach to control testing that permits those sources of variation to be controlled. Figure 1 illustrates a diagram of the laboratory testing system used in this study. The overall dimension and components of the system were similar to those used by Beamer et al. [2005], Heitbrink and Bennett [2006], and Carlo et al. [2010], and they were consistent with European Standard EN 1093-3 [CEN 2006]. A dust collection air handling unit (PSKB-1440, ProVent LLC, Harbor Springs, MI) was used as an air mover for the system. The air handling unit was connected to an automatic tool testing chamber through a 0.3 meter (m) diameter duct about 6.4 m long. A funnel section connected the duct to the automatic tool testing chamber, which had a square cross section of 1.2 m wide and 1.2 m high. A blast gate upstream of the air handling unit was used to adjust the airflow rate passing through the testing system by allowing the excessive air to enter the air handling unit through the gate. Once turned on, the air handling unit was set to draw room air into the testing system at a flow rate of 0.64 m<sup>3</sup>/second (m<sup>3</sup>/sec, equivalent to 1350 CFM). This flow rate was set by manually adjusting the blast gate valve and was monitored by a micromanometer (PVM100 Airflow Developments Ltd., UK) connected to a delta tube (306AM-11-AO, Midwest Instrument, Sterling, MI). The Delta tube functioned as an averaging pitot tube and has four pressure-averaging ports on the front and backside of a tear-shaped or circular cylinder [Miller 1989]. The Delta tube used in this study has a tear-shaped cylinder and it was mounted on the duct about 2.4 m downstream (eight times of the duct diameter) of the funnel section. The accuracy of the flow rate measured by the Delta tube was verified by comparing the flow rate obtained from its manufacturer's calibration equation [Mid-West Instrument, 2004] and that measured by Heitbrink and Bennett [2006] using a 10-point pitot tube traverse of the duct performed in the horizontal and vertical planes (about 0.8% difference).

An aerosol sampling port was open on the duct for mounting a sampling probe of the sampling instrument used in this study. The locations of the Delta tube and sampling port on the duct were chosen to meet the requirements of European Standard EN 1093-3 [CEN 2006] for taking representative samples.

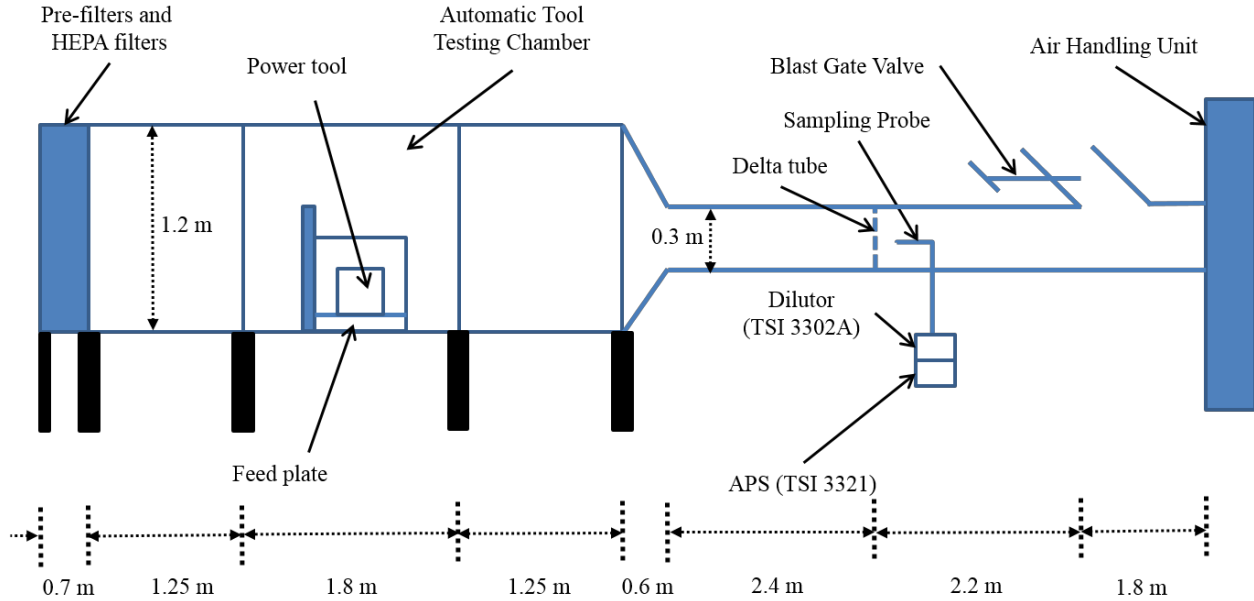


Figure 1. Diagram of the Laboratory Testing System.

The airflow that entered the system first passed through a filter panel, which had the same cross section as the automatic tool testing chamber and was 0.7 m long. The filter panel included one bank of four pre-filters and another bank of four HEPA filters that removed all the particles in the room air so that they did not interfere with the analysis of the dust generated inside the testing system. The filters also helped ensure that the air that entered the system had a uniform velocity profile across the panel's cross section. After the filtration section was the automatic tool testing chamber, which was 4.9 m long and was specifically designed and constructed for this study. Under the operating airflow rate, the flow velocity in the chamber was 0.44 m/sec, which is sufficient to transport respirable dust to the sampling section of the system, according to European Standard EN 1093-3 [CEN 2006]. The Reynolds numbers for the chamber and duct are 34,000 and 170,000, respectively, indicating turbulent flow, which helped maximize mixing to obtain an appropriately representative sample at the sampling section. The air handling unit collected all the dust generated in the testing system with two filter cartridges (P25.20, ProVent LLC, Harbor Springs, MI) before the cleaned air was discharged back into the room.





The walls of the automatic tool testing chamber were transparent so the operation inside could be observed. The chamber featured automatic control using a Programmable Logic Controller (PLC) and a Human Machine Interface (HMI). A circular saw (Model 5057KB, Makita U.S.A., Inc., St. La Mirada, CA) was mounted in

the chamber and fiber-cement saw blades listed in Table 1 were evaluated. The operations of the power tool was controlled using a two-dimensional actuator through the PLC. Fiber-cement siding boards were mounted on a chain-driven feed plate, and the feed rate was automatically controlled through the PLC. Board feed rate and power tool operation were programmed through the HMI so that automatic and repeatable cuts were achieved.

### Saw blades for cutting fiber-cement



PCD blades of 7-1/4 inches (18.4 cm) diameter are the most commonly used in practice for cutting fiber-cement siding based on our previous field surveys. A market search conducted for such blades led to a list that was available for purchase and evaluation in this study. These PCD blades and their specifications are listed in Table 1. The diameter of all the blades is 7-1/4 inches (18.4 cm) and they have a varying number of PCD teeth, except for the Plank Cutter® by MK, which has a continuous rim with embedded diamond tips and a diameter of 7 inches (17.8 cm). The kerf width and shape of each blade also vary according to each model (listed in Table 1).

Table 1. Specifications of fiber-cement saw blades evaluated in the study.

#	Manufacturer	Brand	Model name	Number of teeth	Kerf width	Picture
1	Freud	Diablo	DO704DH	4	0.071	
2	Gila tools	Gila	1037250T04	4	0.087	
3	Gila tools	Gila	1037250T06	6	0.087	
4	Gila tools	Gila	1037250T08	8	0.087	

5	Malco	Malco	FCCB7	4	0.091	
6	Oldham	Oldham	725FC04	4	0.092*	
7	Tenryu	Board Pro	BP-18505	5	0.091	
8	Timberline	Timberline	185-04PCD	4	0.071	
9	CMT orange tools	CMT	236.004.07	4	0.067	
10	Black & Decker	DeWalt	DW3193	6	0.09	
11	Grip-Rite	Grip-Rite	GRFC7144T	4	0.087	
12	Hitachi	Hitachi	18008	4	0.071	

13	Hitachi	Hitachi	18078	8	0.087	
14	Irwin	Marathon	4935473	4	0.071	
15	Ivy classic	Ivy classic	36496	4	0.071	
16	Makita	Makita	A-95124	4	0.087	
17	MK	Plank Kutter®	156994	continuous	DNA	
18	Original	Original	00087	4	0.089*	
19	Oshlun	Oshlun	SBH-072504	4	0.087	
20	PacTool	PacTool	SA707	4	0.087	

21	Task Tools	TASK	T22426	4	0.087	
22	BOSCH	BOSCH	CB704FC	4	0.102	

Note: DNA — Does Not Apply; \* — Measured manually

### Test Conditions

The Makita 5057KB circular saw was applied to test the saw blades listed in Table 1. This saw has an option to attach a dust-collecting box as shown in Figure 2. In this study, we tested each saw blade with the three conditions listed below:

- A. Without control (naked blade)
- B. Capped dust-collecting box (exhaust port capped)
- C. Dust-collecting box plus a passive dust collector (a cyclone and a filter cartridge)

When the dust-collecting box is installed on the saw, the fast-spinning blade induces an airflow, which helps transport a portion of the generated dust to the box, thus reducing the overall dust releasing rate. The exhaust port of the box can be either capped or connected to a dust collector. A capped exhaust port (test condition B) may restrict the induced flow. However, when the exhaust port connects to a passive dust collector (test condition C), the flow is unrestricted. In this study, we assembled the passive dust collector by using a cyclone (model AXD000004, Oneida Air Systems, Inc., Syracuse, NY) and a filter cartridge (part number 90304, Shop-Vac® Corporation, Williamsport, PA) mounted on the cyclone's outlet. In operation, the induced flow from the spinning blade helps transport a portion of the emitted dust into the dust-collecting box. Larger dust particles are collected by the dust-collecting box and the cyclone, and the smaller dust particles are collected by the filter cartridge. We hypothesized that different saw blade designs regarding shape and number of teeth may induce different amounts of airflow, leading to different levels of reduction in dust releasing rates under test conditions B and C. The passive dust collector, which includes the cyclone and air filter, is designed to simulate the operation of the red-spur or the Roan saw described earlier.



**Figure 2. A circular saw (Makita 5057KB) with an on-tool dust-collecting box, and a passive dust collector (a cyclone and a filter cartridge)**

If the outlet of the dust-collecting box is connected to an active dust collector such as a shop vacuum, the airflow provided by the shop vacuum is expected to be much higher than the induced flow by the blade. Therefore, the dust releasing rates would be lower for all evaluated saw blades, so we only tested the shop vacuum with a Diablo saw blade (#1 in Table 1) for comparison with the capped and passive dust controls. For this comparison test, a 12-gallon shop vacuum (model 586-62-11, Shop-Vac® Corporation, Williamsport, PA) was used as the active dust collector. Figure 3 shows circular saw and its connection to the shop vacuum, which came with a disposable filter bag (part number 90662, Shop-Vac® Corporation, Williamsport, PA) to trap most of the dust, and a standard Prolong cartridge filter (part number 90304, Shop-Vac® Corporation, Williamsport, PA) to capture the dust passing through the filter bag. The shop vacuum was rated to provide a 5.66 m<sup>3</sup>/min (200 CFM) flow rate by the manufacturer. However, the actual flow rate can be affected when the shop vacuum is connected to the filters and vacuum hose. More importantly, the flow rate might change due to dust loading on the filter bag

and cartridge filter. A laboratory test found that the flow rate of the LEV was generally in the range of 1.95-2.96 m<sup>3</sup>/min (69-105.8 CFM).



Figure 3. The dust-collecting circular saw and its connection to the shop vacuum.

### Sampling Methods

In this study, the automatic tool testing chamber was set to make a fixed number of repeat cuts of the fiber-cement siding board for each test condition. An Aerodynamic Particle Spectrometer (APS, model 3321, TSI Inc, Shoreview, MN) provided real-time direct reading measurement of the size distribution of the dust generated with a 1-second time resolution. The APS continuously collected an aerosol stream from one of two available duct sampling ports at a 5 Liter per minute (L/min) flow rate. The APS used a time-of-flight technique to measure the aerodynamic diameter of the individually counted particles in the range from 0.5 to 20 micrometers ( $\mu\text{m}$ ). The APS output connected to a computer and the Aerosol Instrument Manager<sup>®</sup> Software (AIM V8.1, TSI Inc., Shoreview, MN) collected and analyzed the APS data. In this study, an isokinetic sampling probe was designed for the APS with a matching flow velocity for the inlet of the sampling probe and the duct. The sampling probe bent 90 degrees and vertically connected to an aerosol



dilutor (model 3302A; TSI Inc, Shoreview, MN), which sat on top of the APS. The dilutor was configured to provide a 100 to 1 dilution so that measurement uncertainty caused by high concentration aerosols was minimized. The dust size distribution directly measured by the APS is based on number concentration, and it can be used to derive the mass concentration of respirable dust by the following equation:

$$C_m = \sum_{i=1}^{52} \frac{\rho_p f_i \pi d_{e,i}^3 N_i}{6 \eta_{dil,i} \eta_{sp,i}} \quad (1)$$

where,

$C_m$  is the mass concentration of respirable dust

$d_{e,i}$  is the equivalent volume diameter of channel  $i$  in the APS and can be calculated by

$$d_{e,i} = d_{a,i} \sqrt{\rho_0 \chi / \rho_p}$$

$d_{a,i}$  is the aerodynamic diameter of channel  $i$  in the APS

$\rho_0$  is the unit density

$\rho_p$  is the density of the dust

$\chi$  is the dynamic shape factor of the dust

$f_i$  is the respirable fraction of the dust with  $d_{a,i}$

$N_i$  is the number concentration of the dust with  $d_{a,i}$

$\eta_{dil,i}$  is the transportation efficiency of the dust with  $d_{a,i}$  through the diluter

$\eta_{sp,i}$  is the transportation efficiency of the dust with  $d_{a,i}$  through the sampling probe

The APS directly measures the aerodynamic diameter of the sampled dust, and it classifies the entire size range into 52 channels with  $d_{a,i}$  representing the aerodynamic diameter for each specific channel  $i$  ( $i = 1-52$ ). In order to obtain the mass of dust in each channel, its density ( $\rho_p$ ) is needed, and its equivalent volume diameter needs to be calculated with the knowledge of its density ( $\rho_p$ ) and dynamic shape factor ( $\chi$ ). In this study, all the dusts generated from cutting fiber-cement siding were assumed to be spherical so their dynamic shape factor was 1. The dust density was also needed for the Stokes correction of the APS data because the APS was calibrated in factory using Polystyrene Latex (PSL) spheres with a density close to 1.05 g/cm<sup>3</sup>. Since the APS measures the aerodynamic diameter in a flow velocity of approximately 150 m/sec instead of still air, the Reynolds numbers of the sampled dusts are outside the Stokes regime; a sizing inaccuracy is caused when the dust density is different from 1.05 g/cm<sup>3</sup>. The Stokes correction for the APS

data can be done by the AIM Software with an input of the dust density. However, it is not straightforward to obtain the actual dust density in this study as the bulk material in fiber-cement siding is a mixture of a few different ingredients, and the density might vary depending on the size of the dust. Thus, the measured board density was used as the dust density. With the assumed dynamic shape factor and density for the sampled dust, the mass concentration of respirable dusts derived from the APS data and Equation (1) could be different from the actual value. However, this difference should be consistent among all the APS data and should not affect the comparison of the releasing rate of respirable dust derived from the APS data under different testing conditions.

In this study, the releasing rate of respirable dust ( $G_{APS}$ ) is defined by the following equation:

$$G_{APS} = \frac{\sum_{t=1}^{T_s} (C_{m,t} Q)}{n_b W} \quad (2)$$

where,

$C_{m,t}$  is the mass concentration of respirable dusts at time  $t$

$Q$  is the volume flow rate in the testing system, 0.64 m<sup>3</sup>/sec

$T_s$  is the total sampling time of the APS for one cut

$n_b$  is the number of boards in the stack, 1 in this report

$W$  is the board width

Since fiber-cement siding in this study was cut by making crosscuts across the board width, the product of  $n_b$  and  $W$  represents the total linear length for one cut. The total linear length cut is commonly used in practice to account for cutting productivity. The APS data contains one set of dust size distribution for every second during the test, which leads to a  $C_{m,t}$  data point for each second using Equation (1). Thus, the summation of  $C_{m,t}Q$  during the sampling time  $T_s$  results in the total mass of respirable dust generated for one cut. The releasing rate of respirable dust defined in Equation (2) represents the mass of respirable dust generated per unit linear length cut.

In this study, the transportation efficiency of dust with  $d_{a,i}$  through the diluter ( $\eta_{dil,i}$ ) was provided by the diluter manufacturer and incorporated within the AIM software. The transportation efficiency through the sampling probe ( $\eta_{sp,i}$ ), however, must be analyzed separately. The loss of dust inside the sampling probe can be attributed to the settling loss in the horizontal part of the probe, the inertial loss at the 90 degree bend, and the diffusion loss throughout the probe. These losses are size dependent so the overall loss of respirable dust depends on the size distribution of

the dust generated during cutting fiber-cement siding. The overall loss of respirable dust was calculated using the equations summarized by Brockman [2011] and the size distribution data from the APS, and it was found to be less than 1% combining all three aforementioned losses. Thus,  $\eta_{sp,i}$  was assumed to be 1 in this study for simplicity.

### **Operating procedure for a cutting test**

Before conducting a cutting test, the automatic tool testing chamber was programmed to perform a pre-determined number of cuts. Each cut included the following steps: 1) the feed plate fed the board; 2) power was supplied to the tool; 3) the 2D actuator moved the tool and made a cut; 4) the tool was turned off; and 5) the 2D actuator moved the tool back to its original position. A waiting time about 5 seconds was programmed between steps 2) and 3) to ensure the blades of the power saw reached the designed rotating speed before making a cut. The sliding speed for the saw, referred to as the cutting feed rate in this report, was set to be 2.54 cm/sec by the PLC.

For each cutting test, the air handling unit was turned on and the flow rate was set to 0.64 m<sup>3</sup>/sec by adjusting the blast gate valve. During each cut, a dust cloud was generated while cutting, and it was carried downstream by the airflow through the tool testing chamber and measured by the instruments through their respective sampling probes on the duct of the testing system. The APS collected size distribution measurements at 1-second intervals. The flow rate in the testing chamber (0.64 m<sup>3</sup>/sec) was optimal so that the APS data with 1-second time resolution captured the entire profile of the dust cloud from each individual cut without overlapping the dust clouds between any two adjacent cuts for all the testing conditions in this study. This ensured the calculation of the respirable dust releasing rate ( $G_{APS}$ ) using Equation (1) for each individual cut. To be consistent, the fiber-cement siding from James Hardie (Mission Viejo, California) was used in all the tests. These boards have width of 8.25 inch (21.0 cm), thickness of 0.30 inch (0.76 cm), and measured density of 1.27±0.01 g/cm<sup>3</sup>.

## **Results and Data Analysis for the Laboratory Evaluation**

Figure 4 shows the size distributions of the dust generated from cutting fiber-cement siding using a Diablo saw blade (#1 in Table 1) with three different engineering control measures. The size distributions represent the dust number concentration per unit width of the instrument's size channel at different aerodynamic diameters. Each data point shown in Figure 4 is the averaged result of five replicates, and the error bars represent the standard deviations of the corresponding data points. The small error bars associated with most data points verify the high repeatability of these tests.

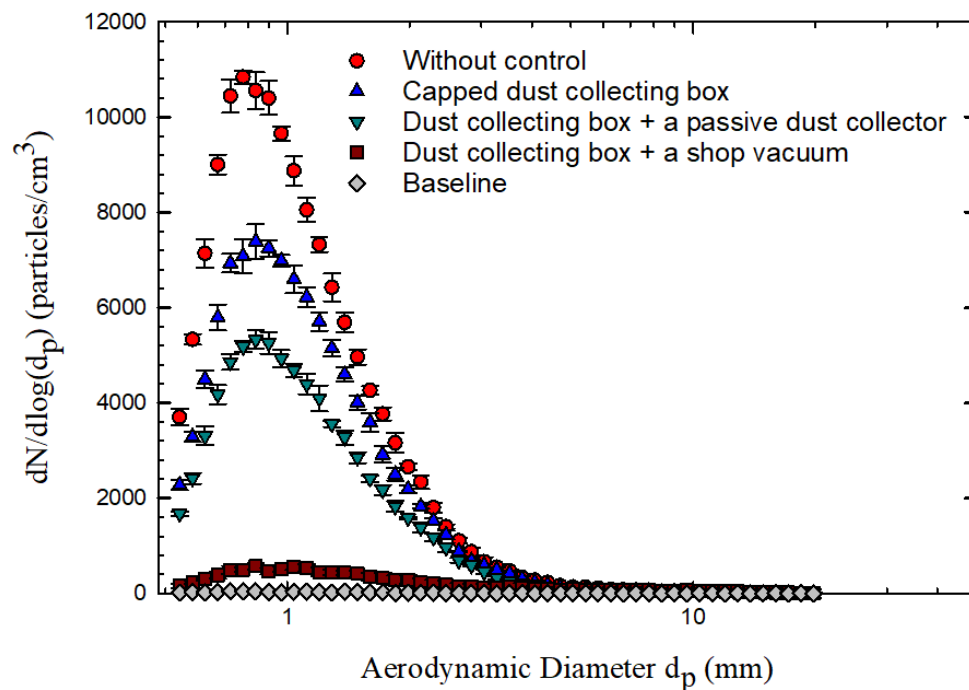


**Figure 4. Number-based size distributions of the dust from cutting fiber-cement siding obtained from the APS.**

The number-based size distributions showed a lognormal distribution with a geometric mean diameter ranging from 0.9-1.1  $\mu\text{m}$  and a geometric standard deviation ranging from 1.5-1.9. However, the total number concentration varied considerably among the four tests. The largest amount of dust was generated when no engineering control was used (test condition A), with an average total number concentration of 10,026 particles/cm<sup>3</sup> as estimated from fitting the data to a lognormal distribution. Dust amount was reduced as different control measures were applied. The test condition B (capped dust-collecting box) and C (dust-collecting box plus a passive dust collector) considerably reduced the dust releasing, with average total number concentrations of 7,040 and 5,003 particles/cm<sup>3</sup>, indicating about 30% and 50% reduction of total particle numbers compared to the concentration from the test condition A. This was achieved by the airflow induced by the blade moving some portion of dust into the box. The test condition C showed better performance due to the restricted airflow for the test condition B with a capped exhaust port. The test with the shop vacuum connected to the exhaust port of the dust-collecting box (Figure 3) resulted in the least amount of dust, 497 particles/cm<sup>3</sup>, which corresponds to a ~95% reduction of total particle numbers from the uncontrolled test condition. This is expected due to the much higher airflow provided by the shop vacuum, and is consistent with the finding from the previous study by Qi et al. [2014] using the Hitachi PCD blade (Model 18008, Hitachi Power Tools, Valencia, CA; #12 in Table 1 and 2) on the

same circular saw. The concentration levels shown in Figure 4 are those monitored in the laboratory setting, which can be very different from those experienced in actual work practice, although the shape of the size distribution is expected to be similar.

Table 2 lists the  $G_{APS}$  computed for the 22 different blades based on Equation (2). The reported  $G_{APS}$  is the average from 5 repeated cuts. The average relative standard deviation (RSD, the ratio of the standard deviation to the average) for all the  $G_{APS}$  data was only 3.3%, demonstrating excellent repeatability of the test; therefore, the standard deviation for each  $G_{APS}$  data is not reported. As shown in the table, the  $G_{APS}$  varies depending on the blade models, ranging from 0.25-1.07 g/m, when no engineering control was applied. The highest  $G_{APS}$ , 1.07 g/m, was found from the Plank Kutter® blade (#17 in Table 1 and 2), which is designed with a continuous rim of diamond tips. The blades with more teeth interact with the fiber-cement board more often per rotation, leading to generating more dust during cutting. Thus, the Plank Kutter® blade is expected to generate the largest amount of dust due to the continuous interaction with the board. Excluding the Plank Kutter® blade, the range of  $G_{APS}$  for the uncontrolled test condition (A) is 0.25-0.50 g/m.

Table 2. Respirable dust releasing rate ( $G_{APS}$ , g/m) from the cutting test for different saw blades

#	Brand	Number of Teeth	Kerf width	Respirable dust releasing rate ( $G_{APS}$ , g/m)			Collection Efficiency (%)
				Without control	Capped dust-collecting box	Dust-collecting box + a passive dust collector	
1	Diablo	4	0.071	0.33	0.26	0.19	41%
2	Gila	4	0.087	0.43	0.37	0.25	43%
3	Gila	6	0.087	0.43	0.37	0.24	45%
4	Gila	8	0.087	0.46	0.40	0.22	53%
5	Malco	4	0.091	0.38	0.33	0.22	42%
6	Oldham	4	0.092*	0.35	0.30	0.16	55%
7	Board Pro	5	0.091	0.37	0.36	0.25	32%
8	Timberline	4	0.071	0.36	0.26	0.17	53%
9	CMT	4	0.067	0.36	0.28	0.18	50%
10	DeWalt	6	0.09	0.45	0.34	0.18	60%
11	Grip-Rite	4	0.087	0.38	0.30	0.20	47%
12	Hitachi	4	0.071	0.29	0.22	0.12	60%

13	Hitachi	8	0.087	0.50	0.37	0.21	58%
14	Marathon	4	0.071	0.44	0.35	0.22	51%
15	Ivy classic	4	0.071	0.35	0.28	0.18	48%
16	Makita	4	0.087	0.33	0.30	0.20	39%
17	Plank Kutter®	continuous	DNA	1.07	0.88	0.57	47%
18	Original	4	0.089*	0.25	0.27	0.19	26%
19	Oshlun	4	0.087	0.45	0.36	0.22	52%
20	PacTool	4	0.087	0.38	0.27	0.14	63%
21	TASK	4	0.087	0.47	0.32	0.16	66%
22	BOSCH	4	0.102	0.41	0.37	0.29	29%

Note: DNA — Does Not Apply; \* — Measured manually

The  $G_{APS}$  generally decreases as control measures are applied. With the capped dust-collecting box attached to the circular saw (test condition B), the range of  $G_{APS}$  was reduced to 0.22-0.40 g/m (excluding the Plank Kutter® blade). It was further reduced to 0.12-0.29 g/m when the passive dust collector was connected to the dust-collecting box (test condition C). The dust releasing varies noticeably with different blade models among all the three test conditions. The performance of the two passive control measures seems to depend on the characteristics of blades such as their shape and number of the teeth as they may affect the induced airflow. Therefore, a collection efficiency ( $\eta$ ) is defined in Equation (3) to serve as an indicator of how well the induced flow from different blade designs help collect the dust into the dust-collecting box and passive dust collector, thus reducing  $G_{APS}$ .

$$\eta = 1 - \frac{G_{APS, \text{test condition C}}}{G_{APS, \text{test condition A}}} \quad (3)$$

As shown in Table 2, the collection efficiency varies with the blade models ranging from 26% to 66%.

The average  $G_{APS}$  with different kerf widths is listed in Table 3. Please note that only the blades with 4 teeth are included for this comparison. If other blade characteristics (such as number of teeth and shape) remain the same, the blade with larger kerf width is expected to generate more dust due to its larger contact area and larger material removed from the fiber-cement board. However, the blades tested vary greatly on their shape designs, making it difficult to assess the effect of kerf width on  $G_{APS}$ . Therefore, we categorized the blades into two groups with one group having kerf width smaller than 0.085 inch and another group with larger kerf width. The results reported in Table 3 clearly show that the average  $G_{APS}$  increased with the kerf width for all the three test conditions. However, the difference is not statistically significant ( $P$  value > 0.01 as reported in Table 3).

Table 3. Average respirable dust releasing rate ( $G_{APS}$ , g/m) from the fiber-cement saw blades having a kerf width smaller or larger than 0.085 inches

Kerf with (inches)	Respirable dust releasing rate ( $G_{APS}$ , g/m)		
	Without control	Capped dust collecting box	Dust collecting box + a passive dust collector
smaller than .085	0.35	0.28	0.18
larger than .085	0.38	0.32	0.20
<i>P</i> value	0.16	0.03	0.10

We also investigated the effect from the number of teeth on a blade on  $G_{APS}$  by categorizing the blades and their  $G_{APS}$  results into three groups, with 4, 6 and 8 teeth on the blade, respectively. The results are listed in Table 4. In general, blades having more teeth show higher  $G_{APS}$ , which is expected because of more cutting interactions between the blade teeth and the fiber-cement board. However, this effect seems to be reduced for the conditions with the passive dust controls. A plausible explanation is that although more teeth on the blade generated more dust, they also induced a higher airflow rate, resulting in more dust being transported to the dust-collecting box and the passive dust collector. This is also evidenced by the higher collection efficiency related to the larger number of teeth (listed in Table 4). In fact, when further examining the three Gila blades, which have 4, 6, and 8 teeth and the same other blade characteristics, the  $G_{APS}$  decreased with the number of teeth when the passive dust collector was used.

Table 4. Average respirable dust releasing rate ( $G_{APS}$ , g/m) from the fiber-cement saw blades having different number of tooth

Number of tooth	Respirable dust releasing rate ( $G_{APS}$ , g/m)			Collection Efficiency (%)
	Without control	Capped dust collecting box	Dust collecting box + a passive dust collector	
4	0.37	0.30	0.19	48%
6	0.40	0.33	0.20	49%
8	0.48	0.38	0.22	55%

The data listed in Table 2 shows that the 4-teeth Hitachi blade (#12) has the lowest dust releasing rate under the two test conditions with passive controls. Fewer teeth, thinner kerf, and its specific design characteristics may contribute to its lower dust releasing rate. This blade also has one of the highest collection efficiencies at 60%, indicating that its design is helpful in inducing airflow and transporting dust into the subsequent dust collectors. More specifically, it has a semi-circular gullet with the non-tooth side having a smoother curve leading to the blade’s rim, which seems to

be on the same circumference as the other side of the gullet (Figure 5). Such a “smooth” gullet may be at an optimized balance between inducing airflow and transporting the dust into the dust collectors. This hypothesis is evidenced by the relatively high collection efficiency for the blades with a similar “smooth” gullet design (#9, #10, #11, #13, #14, #19, #20, #21 in Table 1 and Table 2).



Figure 5. Pictures of (a) saw blades (#7, #12, #18, and #22 from the left) and (b) Enlarged tooth pictures for comparison

Figure 5 also shows the gullet design for three other blades, which have the lowest collection efficiency. The gullet of the Board Pro blade (#7) is almost a  $\frac{3}{4}$  circle. It is apparent that such a “circled” design is not good for inducing airflow because it encloses the space. The gullet of the Original blade (#18) is “flat” on its non-tooth side. Since the gullet is less enclosed, it may induce more airflow. However, it may be too open to keep the generated dust in the induced flow, resulting in less dust transported to the dust collector. The Bosch blade (#22) has its PCD tip protruding considerably beyond the rim of the other side of the gullet. With such a design, generated dust may easily disperse in all directions without being captured by the induced airflow. Overall, the lower collection efficiency for these three blades may attribute to their gullet designs.

The  $G_{APS}$  for the Diablo blade (#1 in Table 1 and 2) used with the shop vacuum test is  $0.06 \pm 0.03$  g/m. The relative larger RSD for this particular test is due to lower particle count, thus larger counting uncertainty in the APS. In comparison, the average  $G_{APS}$  for the 4-tooth Hitachi blade (#12 in Table 1 and 2) used in the same saw was reported at 0.03 g/m under a LEV rate of  $2.54 \text{ m}^3/\text{min}$  (90 CFM) [Qi et al. 2014]. The lower  $G_{APS}$  for the 4-tooth Hitachi blade is consistent with the results shown in Table 2.

## Discussion

The test results clearly show that blade design affects the dust generation as well as the dust collection by the passive dust control measures. The uncapped dust-collecting box does not lead to satisfactory dust collection. However, after adding



the passive dust collector, it results in considerably higher dust collection, with a collection efficiency as high as 66%. In theory, the collection efficiency could translate into similar amount of exposure reduction compared to the uncontrolled exposure.

The average  $G_{APS}$  for the Diablo blade used with the passive dust collector (0.19 g/m) is 3.2 times higher than the average  $G_{APS}$  when it was used with the shop vacuum (0.06 g/m). Since the passive dust collector is to simulate the operation of the red-spur saw, we compared the data from the two field surveys when the same Diablo blades were used with both the Makita circular saw with shop vacuum and the red-spur saw [Qi and Echt, 2014; Qi and Garcia, 2014]. The average 8-hr TWA exposure when using the red-spur saw ( $0.060 \pm 0.039$  mg/m<sup>3</sup> from 6 samples) was 4.0 times higher than that for the Makita saw with shop vacuum ( $0.015 \pm 0.012$  mg/m<sup>3</sup> from 9 samples). The results suggests that the comparison of the average  $G_{APS}$  found from the laboratory evaluation for the two control measures (dust-collecting box plus passive dust collector versus shop vacuum) is in reasonably good agreement with that of their corresponding average 8-hr TWA exposures obtained from the field surveys.

The 4-tooth Hitachi blade (#12 in Table 1 and 2) exhibited the lowest  $G_{APS}$  when using the passive dust collector (0.12 g/m), which is only 63% of the average  $G_{APS}$  for the diablo blade under the same testing condition (0.19 g/m). Additional blade design improvements with optimized gullet may be considered for higher induced airflow and better dust transportation into the dust collector. With an improved blade design, it is possible to considerably reduce the 8-hr TWA exposure from the level found from the red-spur saw with the Diablo blade ( $0.060 \pm 0.039$  mg/m<sup>3</sup>) using a similar on-tool passive dust collector, thus possibly meeting the NIOSH REL and OSHA PEL (0.05 mg/m<sup>3</sup>). Such an engineering control measure, once validated from field surveys, may be an alternative to the one using a shop vacuum. Although it may be difficult to reduce the exposure to the same level as the control of using a shop vacuum, the control of using an on-tool passive dust collector would provide the benefit of avoiding carrying an additional shop vacuum and its hose during the work.

## Conclusions/Recommendations

Controlling exposures to occupational hazards is the fundamental method of protecting workers. Traditionally, a hierarchy of controls has been used as a means of determining how to implement feasible and effective controls. One representation of the hierarchy of controls can be summarized as follows:

- Elimination
- Substitution
- Engineering Controls (e.g. ventilation)
- Administrative Controls (e.g. reduced work schedules)
- Personal Protective Equipment (PPE) (e.g. respirators)

The idea behind this hierarchy is that the control methods at the top of the list are potentially more effective, protective, and economical over time than those at the bottom. Following the hierarchy normally leads to the implementation of inherently safer systems, ones where the risk of illness or injury has been substantially reduced.

The results of laboratory test revealed that the dust releasing rate, i.e.,  $G_{APS}$ , generally increases with the number of teeth and the kerf width of the blades. The blade with a continuous rim of tips (Plank Cutter® blade, #17 in Table 1 and 2) generated the highest amount of dust. The effect of the number of blade teeth was greatly reduced when the passive dust control measures were used, possibly because more teeth may induce a higher airflow rate while generating more dust.

The passive dust control measures of using a capped dust-collecting box and the box with a passive dust collector both led to certain amounts of dust collection. The control measure with the passive dust collector provided a dust collection efficiency as high as 66% depending on the blade design. The 4-tooth Hitachi blade (#12 in Table 1 and 2) resulted in the lowest dust releasing rate with the two passive dust control measures. The gullet design of the blade seems to play an important role affecting the amount of dust generation as well as the collection efficiency of the passive dust controls. Based on the exposure data from previous field surveys using the red-spur saw, additional improvement on blade designs is possible to reduce the 8-hr TWA exposure to RCS below the NIOSH REL and OSHA PEL while cutting fiber-cement siding using a circular saw with on-tool dust collectors similar to the one used in the red-spur saw. Further investigation will be needed to improve the blade design with the passive dust control measure, and to validate its performance through field studies.

## References

81 Fed. Reg. 16285 [2016]. Occupational Safety and Health Administration: occupational exposure to respirable crystalline silica; final rule. (To be codified at 29 CFR 1926.1153).

ACGIH [2016]. 2016 TLVs® and BEIs®: threshold limit values for chemical substances and physical agents and biological exposure indices. Cincinnati, OH: American Conference of Governmental Industrial Hygienists.

Akbar-Khanzadeh F, Brillhart RL [2002]. Respirable crystalline silica dust exposure during concrete finishing (grinding) using hand-held grinders in the construction industry. *Ann Occup Hyg* 46:341-346.

Beamer BR, Shulman S, Maynard A, Williams D, Watkins D [2005]. Evaluation of misting controls to reduce respirable silica exposure for brick cutting. *Ann Occup Hyg* 49(6):503-10.

Bousquin J [2009]. Fiber cement's aesthetics and durability continue to gain fans. Building Products Magazine. Publication date: February 13, 2009. [<http://www.ebuild.com/articles/875202.hwx>. Accessed 2 August 2016.

Brockman [2011]. Aerosol transport in sampling lines and inlets. In: Kulkarni P, Baron PA, Willeke K eds, Aerosol measurement-principles, techniques, and application. New Jersey: John Wiley & Sons, pp 69-105.

Bureau of Mines [1992]. Crystalline silica primer. Washington, DC: U.S. Department of the Interior, Bureau of Mines, Branch of Industrial Minerals, Special Publication.

Carlo RV, Sheehy J, Feng HA, Sieber WK [2010]. Laboratory evaluation to reduce respirable crystalline silica dust when cutting concrete roofing tiles using a masonry saw. J Occup Environ Hyg 7(4):245-51.

CEN [2006]. EN 1093-3, Safety of machinery-Evaluation of the emission of airborne hazardous substances-Part 3: Test bench method for measurement of the emission rate for a given pollutant. Brussels: European Committee for Standardization.

Chisholm J [1999]. Respirable dust and respirable silica concentrations from construction activities. Indoor Built Environ 8:94-106.

Flanagan ME, Seixas N, Majar M, Camp J, Morgan M [2003]. Silica dust exposures during selected construction activities. AIHA Journal 64: 319-328.

Glindmeyer HW, Hammad YY [1988]. Contributing factors to sandblasters' silicosis: inadequate respiratory protection equipment and standards. J Occup Med 30: 917-921.

Heitbrink WA, Bennett J [2006]. A numerical and experimental investigation of crystalline silica exposure control during tuck-pointing. J Occup Environ Hyg 3: 366-378.

Linch, KD [2002]. Respirable concrete dust-silicosis hazard in the construction industry. Appl Occup Environ Hyg 17: 209-221.

Lofgren DJ, Johnson DC, Walley TL [2004]. OSHA Compliance issues: silica and noise exposure during installation of fiber-cement siding. J Occup Environ Hyg 1: D1-D6.

Mid-West Instrument [2004]. Delta-Tube: application and system design data. Sterling Heights, MI: Mid-West Instruments, Bulletin No. ASDE/04. <http://www.midwestinstrument.com/pdfs/bulletins/DeltaTubeBulletinNo.ASDE04.pdf>

Miller RW [1989]. Flow measurement engineering handbook. 2<sup>nd</sup> Edition. New York; McGraw-Hill.

Nash NT, Williams DR [2000]. Occupational exposure to crystalline silica during tuckpointing and the use of engineering controls. *Appl Occup Environ Hyg* 15:8–10.

NIOSH [1986]. Occupational respiratory diseases. Cincinnati, OH: U.S. Department of Health and Human Services, Public Health Service, Centers for Disease Control, National Institute for Occupational Safety and Health, DHHS (NIOSH) Publication No. 86-102.

NIOSH [2002]. NIOSH Hazard Review: Health Effects of Occupational Exposure to Respirable Crystalline Silica. Cincinnati, OH: U.S. Department of Health and Human Services, Public Health Service, Centers for Disease Control and Prevention, National Institute for Occupational Safety and Health, DHHS (NIOSH) Publication No. 2002-129.

Qi C, Echt A, See M [2013]. In-Depth Survey Report: Partnering to Control Dust from Fiber-Cement Siding. DHHS/CDC/NIOSH Cincinnati, OH. Report No. EPHB 358-11a. <https://www.cdc.gov/niosh/surveyreports/pdfs/358-11a.pdf>

Qi C, Echt A [2014]. In-Depth Survey Report: Partnering to Control Dust from Fiber-Cement Siding. DHHS/CDC/NIOSH Cincinnati, OH. Report No. EPHB 358-13a. <https://www.cdc.gov/niosh/surveyreports/pdfs/358-13a.pdf>

Qi C, Garcia A M [2014]. In-Depth Survey Report: Partnering to Control Dust from Fiber-Cement Siding. DHHS/CDC/NIOSH Cincinnati, OH. Report No. EPHB 358-14a. <https://www.cdc.gov/niosh/surveyreports/pdfs/358-14a.pdf>

Qi C, Echt A, Gressel M [2014]. In-Depth Survey Report: Partnering to Control Dust from Fiber-Cement Siding. DHHS/CDC/NIOSH Cincinnati, OH. Report No. EPHB 358-16a. <https://www.cdc.gov/niosh/surveyreports/pdfs/358-16a.pdf>

Rappaport SM, Goldberg M, Susi P, Herrick RF [2003]. Excessive exposure to silica in the U.S. construction industry. *Ann Occup Hyg* 47:111-122.

Thorpe A, Ritchie AS, Gibson MJ, Brown RC [1999]. Measurements of the effectiveness of dust control on cut-off saws used in the construction industry. *Ann Occup Hyg* 43:443-456.

US Census Bureau [2013]. SURVEY OF CONSTRUCTION, Principle Type of Exterior Wall Material of New One-Family Houses Completed. <http://www.census.gov/const/C25Ann/sftotalexwallmat.pdf>. Accessed November 9, 2016.

Woskie SR, Kalil A, Bello D, Virji MA [2002]. Exposures to quartz, diesel, dust, and welding fumes during heavy and highway construction. *AIHA Journal* 63:447-457.

**Delivering on the Nation's promise:  
Promoting productive workplaces through  
safety and health research**

**Get More Information**

Find NIOSH products and get answers to workplace safety and health questions:

1-800-CDC-INFO (1-800-232-4636) | TTY: 1-888-232-6348

CDC/NIOSH INFO: [cdc.gov/info](https://www.cdc.gov/info) | [cdc.gov/niosh](https://www.cdc.gov/niosh)

Monthly *NIOSH eNews*: [cdc.gov/niosh/eNews](https://www.cdc.gov/niosh/eNews)